

Dislocation Generation in the Two-Dimensional Frenkel-Kontorova Model at High Stresses

P. S. Lomdahl and D. J. Srolovitz

Los Alamos National Laboratory, Los Alamos, New Mexico 87545

(Received 21 April 1986)

Dislocation generation is studied in a generalized two-dimensional Frenkel-Kontorova model which allows consideration of dislocations of arbitrary Burgers vector and line shape. Two new mechanisms for dislocation generation at high stresses have been found: (1) heterogeneous nucleation of dislocations on preexisting dislocations and (2) generation of dislocation loops in the wake of a moving dislocation. These new mechanisms provide an understanding of how materials generate the density of dislocations required to accommodate arbitrary strains at high strain rates.

PACS numbers: 61.70.Ga, 03.40.Kf, 61.70.At, 62.20.Fe

For stresses larger than the macroscopic yield stress of a crystalline material, deformation is controlled by the generation and propagation of dislocations.¹ In crystals deformed at high stresses, the dislocation density tends to adjust itself in such a way as to accommodate the applied strain. While a number of mechanisms for dislocation generation have been proposed and observed at low strain rates, they do not account for deformation processes occurring at high rates.² This lack of understanding may be traced to our inadequate models of dislocation dynamics which have been limited to zero-dimensional or continuum descriptions of dislocations.^{1,3,4}

In this Letter, we examine mechanisms for dislocation generation under extreme conditions. We find that at high stresses and temperatures, dislocations nucleate *heterogeneously* on preexisting dislocations. This new result is obtained in the framework of a Frenkel-Kontorova (FK) model⁵ which we have generalized to two spatial dimensions so that transverse effects are included systematically.⁶ We perform finite-temperature molecular-dynamics simulations on a two-dimensional discrete lattice. The ability of the dislocation to deform arbitrarily is an essential aspect of dislocation multiplication. We are able to treat not only edge dislocations but dislocations of arbitrary Burgers vector, including screw dislocations which are strictly transverse defects. While dislocation stress fields decay as $1/r$, the stress fields in the FK model decay exponentially. This deficiency is of little consequence since dislocation dynamics is controlled by the core which is properly accounted for in the FK model.

The 1D FK model^{4,5,7,8} has been used extensively as a description of a variety of physical systems. However, the zero-dimensional nature of defects limits its utility as a paradigm for systems where the defects are one dimensional. While the present 2D results are couched in the language of dislocation dynamics, the methods applied and many of the conclusions drawn should also be appropriate for descriptions of defects in other systems, e.g., weakly pinned charge-density waves,⁹ commensurate-incommensurate transitions,¹⁰ and domain-wall dynamics in magnetic media.¹¹

The Hamiltonian of the 2D FK model may be written as $H_{FK} = H_{kin} + H_{lat} + H_{pot} + H_F$, where

$$H_{kin} = \sum_{i,j} \frac{1}{2} M (\dot{u}_{i,j}^2 + \dot{v}_{i,j}^2), \quad (1a)$$

$$H_{lat} = \sum_{i,j} \frac{1}{2} k [(l_x - 2\pi)^2 + (l_y - 2\pi)^2], \quad (1b)$$

$$l_x^2 = (u_{i,j} - u_{i+1,j} - 2\pi)^2 + (v_{i,j} - v_{i+1,j})^2,$$

$$l_y^2 = (u_{i,j} - u_{i,j+1})^2 + (v_{i,j} - v_{i,j+1} - 2\pi)^2,$$

$$H_{pot} = \sum_{i,j} \alpha [2 - \cos(u_{i,j}) - \cos(v_{i,j})], \quad (1c)$$

$$H_F = \sum_{i,j} f_x u_{i,j} + f_y v_{i,j}. \quad (1d)$$

Here the equilibrium lattice spacing is 2π and $u_{i,j}$ and $v_{i,j}$ are the displacements of atom i,j in the x and y directions, respectively. H_{lat} is the energy stored in the square lattice of springs which connects each atom to its nearest neighbors. The terms l_y and l_x are the lengths of the springs connecting an atom to its nearest neighbors. We have taken the mass $M=1$, the spring constant $k=1$, thus defining the time unit $[(M/k)^{1/2}=1]$. The term H_{pot} is our generalization to 2D of the usual FK substrate potential and thus models the influence of the layer of atoms below our plane. The strength of the potential, α , was chosen as $\frac{1}{3}$ to correspond to a Poisson ratio of $\frac{1}{3}$ (a typical value for a metal). Here we have assumed that the interatomic spacing in the plane is equal to the interplane separation. H_F has been added to the Hamiltonian to facilitate the inclusion of applied stresses. Since a force is applied only to the atoms connected by springs, forces in the x and y directions (f_x and f_y) correspond to shear stresses σ_{xz} and σ_{yz} , respectively.

The equations of motion for $u_{i,j}$ and $v_{i,j}$ are obtained from (1) and Hamilton's equations in the usual way. To describe the interaction with a thermal reservoir at temperature T , damping and noise forces have been added to the equations of motion: $F_{i,j}^\mu = -M\Gamma\dot{u}_{i,j} + \eta_{i,j}^\mu(t)$ and

$F_{ij}^v = -M\Gamma\dot{v}_{ij} + \eta_{ij}^v(t)$. We have taken the correlation function for the random forces to be $\langle \eta_{ij}^v(t)\eta_{i'j'}^v(t') \rangle = 2M\Gamma k_B T \delta_{i,i'} \delta_{j,j'} \delta(t-t')$, where θ is either u or v and k_B is Boltzmann's constant. The effect of the two terms is to bring the system to thermal equilibrium, which of course only is meaningful when $f_x = f_y = 0$. The damping constant Γ was chosen such that the lowest-frequency (nonzero) phonon in our 90×90 system is substantially underdamped (i.e., $\Gamma = 0.005$). Periodic boundary conditions were used. The stochastic equations of motion were solved by a molecular-dynamics technique developed by Greenside and Helfand.¹² All runs were allowed to equilibrate at the appropriate temperature prior to the application of the stresses. All energies and temperatures are measured in units where the maximum of the potential is $4a$.

The two basic excitations in this model are edge and screw dislocations. These defects are schematically illustrated in Fig. 1. The diagonal springs in Fig. 1(b) represent a consistent picture of the displacement discontinuity observed along the slip plane of a screw dislocation in a 3D crystal. An edge is defined as a dislocation where the Burgers vector \mathbf{b} is perpendicular to the dis-

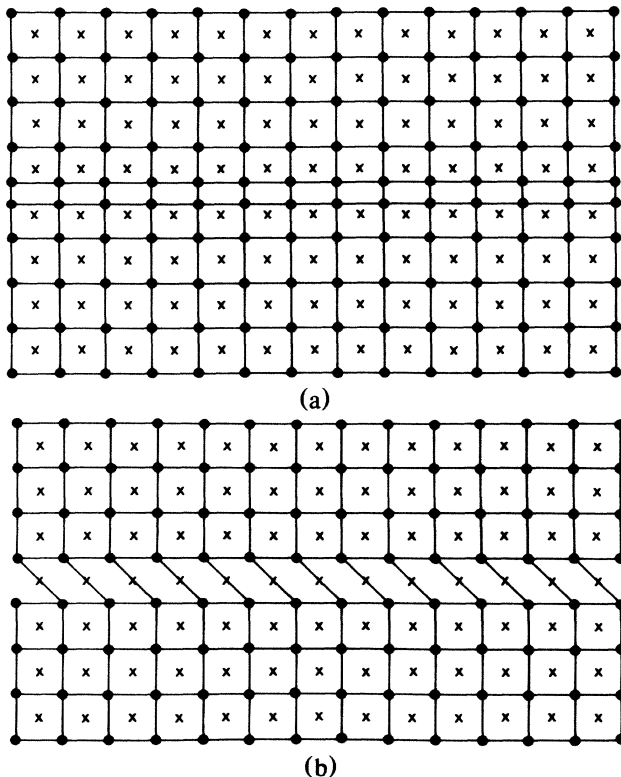


FIG. 1. Excitations in the 2D FK model: (a) The edge dislocation $\mathbf{b}/2\pi = [0,1]$, and (b) the screw dislocation, $\mathbf{b}/2\pi = [1,0]$, where the dislocation lines are parallel to the x axis. The crosses correspond to maxima in the substrate potential, the solid dots represent the particle positions, and the solid lines connecting particles represent the springs.

location line. Similarly, a screw is a dislocation where \mathbf{b} is parallel to the dislocation line. In principle, however, for any \mathbf{b} the dislocation line may be of arbitrary orientation and hence a dislocation may have both edge and screw character. In our studies of the dynamics of straight dislocations we have found a pronounced asymmetry in the minimum force (stress) required to move a dislocation (i.e., a Peierls barrier). The Peierls barrier for an edge dislocation^{8,13} in our model is $\sigma \approx 10^{-7}$, while for a screw dislocation the barrier corresponds to $\sigma \approx 0.1$, where the shear modulus is $\mu = 4\pi^2/3 \approx 13.2$. Asymmetries in the Peierls barriers are commonly observed in bcc metals (although smaller than found here) and have been attributed to the geometry of the dislocation core.¹⁴ Even though the Peierls barrier is sensitive to the value of a ,^{8,13} the physical mechanisms presented below are insensitive to the particular choice of a .

In addition to the Peierls barrier, the dislocation-line energy (per unit length) also depends on the relative orientation of the Burgers vector. This dependence is indicated in Table I for dislocations oriented parallel to the x axis. The energies were calculated from (1) with $H_F = 0$. The energy of the edge exceeds that of the screw by a factor of approximately 7.¹⁵ When a screw and edge are combined such that $\mathbf{b}/2\pi = [1,1]$, the line energy of the resultant dislocation is close to that of the infinitely separated, static screw and edge. This shows that to lowest order the elastic fields of the screw and edge do not couple. However, when the screw and edge are very close together, the higher-order terms in the Hamiltonian may become important. This is strikingly demonstrated in the case of $\mathbf{b}/2\pi = [1,-1]$, where the resultant line energy is identically zero. This dislocation corresponds to two lines of atoms which lie exactly on top of one another and across which the lattice is shifted by 2π parallel to the line. All of the atoms lie at the bottom of wells and all springs are at their equilibrium length; therefore this dislocation has zero energy. In atomic systems such situations are prevented by hard-core atomic repulsions. The energy of the system is thus unchanged upon collapse from two to one dimension, but this is generally prevented by application of appropriate boundary conditions.

While dislocation generation via homogeneous nucleation does not occur at significant rates in 3D crystals, we find that dislocations can be readily generated via *heterogeneous* nucleation. In Fig. 2 we show the genera-

TABLE I. Dislocation energies per unit length.

$\mathbf{b}/2\pi$	Energy
$[1,0],[1,0]$	0.662
$[0,1],[0,-1]$	4.597
$[1,1],[1,1]$	6.381
$[1,-1],[1,-1]$	0

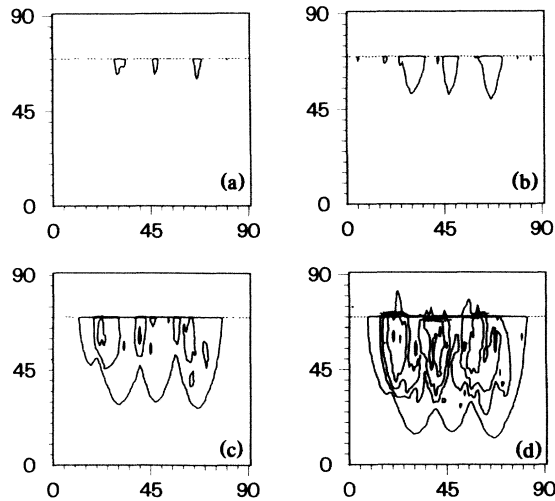


FIG. 2. Dislocation generation on a static screw dislocation (dashed line). The applied force and temperature are $f_y = 0.175$ and $T = 0.15$. The solid lines corresponds to dislocations with $\mathbf{b}/2\pi = [0,1]$. (a)–(d) Times of 17.5, 30, 55, and 70, respectively.

tion and temporal evolution of dislocations nucleated on a preexisting static screw dislocation ($\sigma_{yz} = 0.175 \approx \mu/75$ and $T \approx 0.15$). The dislocation lines are drawn where the displacement field is equal to π (or an odd multiple thereof), thus indicating the center of the dislocation. Several dislocation loops are seen to nucleate heterogeneously, but with \mathbf{b} perpendicular to that of the preexistent screw and parallel to the direction of the applied force. As time progresses, these dislocation loops grow, eventually merging and forming much larger loops. During this period of growth additional loops nucleate. The dislocation loops appear to have preferentially nucleated at kinks on the screw dislocation. We have observed similar results where the initial, static dislocation was an edge.

The loops in Fig. 2 grow preferentially in the direction perpendicular to the static screw dislocation because of the much lower Peierls barrier for edges than screws. The faster motion of the edge segments of the loop results in an increased density of screw dislocations. Since the energy of the dislocation containing both edge and screw components depends on the relative signs of the edge and screw, the loops nucleate on only one side of the screw.

While the upper portion of the loop remains static, only the section of the loop away from the screw grows. The preexisting screw dislocation thus acts as a barrier to the passage of the other dislocations. While the applied stress used in the simulation shown in Fig. 2 is insufficient to separate the edge from the screw, once three concentric loops have nucleated [Fig. 2(d)], the stress field due to the dislocation pileup¹ is sufficient to cause

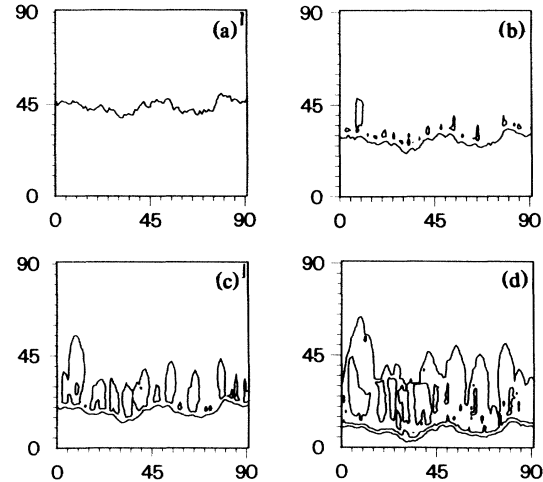


FIG. 3. Dislocation generation behind an edge dislocation moving under the influence of an applied force $f_y = 0.175$ and $T = 0.15$ at times (a) 0, (b) 20, (c) 30, and (d) 40.

the first edge dislocation to dissociate from the screw. To our knowledge, the prediction of heterogeneous nucleation of dislocations on other dislocations has not previously been made since continuum elastic theories are incapable of describing the details of the interactions around the dislocation core.

While the mechanism of heterogeneous nucleation of dislocations described above relies on the fact that it is easier to nucleate a dislocation in a region of the crystal which is already distorted by other dislocations, dislocations may also be heterogeneously nucleated when that distortion is caused by phonons. For example, when a straight dislocation approaches the speed of sound, the phonons emitted are of sufficient amplitude to create a pair of dislocations of opposite signs (this conserves net Burgers vector).^{1,3,4,8} This phenomenon is known as dislocation breakdown. We observe a similar phenomenon when the dislocation is not constrained to remain straight and is roughened by thermal fluctuations. In Fig. 3, we show an example of such a case where dislocation loops are being emitted behind a moving dislocation at a finite temperature ($\sigma_{yz} = 0.175 \approx \mu/75$ and $T \approx 0.15$). In this case, the stress moving the dislocation was insufficient to cause either dislocation breakdown or the homogeneous nucleation of dislocation loops.

As the temperature of the system is raised, the equilibrium roughness of a dislocation line increases. This increased roughening causes the dislocation to pinch off loops, which will decay in the absence of an applied stress. While the application of a stress may allow those loops to expand, an applied stress sufficient to move the dislocation will result in the absorption of the loops ahead of the moving dislocation. Further, a focusing effect due to the superposition of phonons from different

sections of the temperature-roughened dislocation will increase the local loop nucleation rate. Therefore, at sufficiently high temperatures and stresses, a moving dislocation will leave expanding dislocation loops in its wake, as seen in Fig. 3.

Mechanisms for dislocation generation have been known for decades (e.g., Frank-Read source, pole mechanisms),¹ but they require the formation of special spatial configurations. At elevated temperatures and stresses, additional mechanisms for the production of dislocations are possible. We have demonstrated two such mechanisms which are subsets of what we label the heterogeneous nucleation of dislocations. In both cases the heterogeneities responsible for nucleation are preexisting dislocations. In one case the nucleation occurred on static dislocations, but it can also happen as a strictly dynamic effect. Unlike other mechanisms for dislocation generation, all dislocations in the crystal are potential nucleation sites. Hence, while other generation mechanisms may operate with greater frequency, these new mechanisms for dislocation generation may dominate because of their much greater density. Although the Frenkel-Kontorova model is a simplistic description of atomic interactions in a crystal, its generalization to two dimensions contains the essential physics to capture the qualitative behavior of single- and multiple-dislocation phenomena such as dislocation breakdown, dislocation-impurity interactions, and dislocation pileups.

¹J. P. Hirth and J. Lothe, *Theory of Dislocations* (Wiley, New York, 1968).

²J. N. Johnson, O. E. Jones, and T. E. Michaels, *J. Appl.*

Phys. **41**, 2330 (1970); Y. M. Gupta, G. E. Duvall, and G. R. Fowles, *J. Appl. Phys.* **46**, 532 (1975); G. Meir and R. J. Clifton, *J. Appl. Phys.* **59**, 124 (1986).

³See, e.g., *Dislocation Dynamics*, edited by A. R. Rosenfield, G. T. Hahn, A. L. Bement, and R. I. Jaffee (McGraw-Hill, New York, 1967).

⁴J. H. Weiner, in *The Mechanics of Dislocations*, edited by E. C. Aifantis and J. P. Hirth (American Society for Metals, Metals Park, OH, 1985), p. 5.

⁵J. Frenkel and T. Kontorova, *Phys. Z. Sowj.* **13**, 1 (1938); [*J. Phys. (Moscow)* **1**, 137 (1939)].

⁶Other generalizations of the FK model to higher dimensions have been attempted, e.g., W. T. Sanders, *J. Appl. Phys.* **36**, 2822 (1965). These approaches yield coupled 1D FK models and hence the displacement variable is a scalar. A true generalization to 2D must involve a vector field.

⁷S. Aubry, in *Solitons in Condensed Matter Physics*, edited by A. R. Bishop and T. Schneider (Springer, Berlin, 1978), p. 264.

⁸M. Peyrard and M. D. Kruskal, *Physica (Amsterdam)* **13D**, 88 (1984).

⁹For a review, see *Charge Density Waves in Solids*, edited by G. Hutiray and J. Solyom, *Lecture Notes in Physics* Vol. 217 (Springer, Berlin, 1985).

¹⁰See, e.g., P. Bak, *Rep. Prog. Phys.* **45**, 587 (1982).

¹¹See, e.g., F. H. de Leeuw *et al.*, *Rep. Prog. Phys.* **43**, 689 (1980).

¹²H. S. Greenside and E. Helfand, *Bell. Syst. Tech. J.* **60**, 1927 (1981).

¹³R. H. Hobart, *J. Appl. Phys.* **36**, 1944 (1965).

¹⁴V. Vitek, *Cryst. Lattice Defects* **5**, 1 (1974); see also Ref. 1, p. 371.

¹⁵This ratio is larger than in a 3D elastic system by approximately a factor of 5 since the FK model only induces core effects and has no long-range elastic field.